

## LOW-ENERGY ION FLOWS INTO THE MAGNETOSPHERE

M. Lockwood

*Rutherford Appleton Laboratory, Chilton, Didcot, OX11 0QX,  
U.K.*

### ABSTRACT

Ion flows from the ionosphere into the magnetosphere fall into two main categories: cold (<1eV), "classical" polar wind and heated (>1eV), suprathermal ion outflows. A wealth of new understanding of these outflows has resulted from the Dynamics Explorer Mission. This review describes both the confirmation of the predicted classical polar wind as well as the revelation of a great variety of low-energy suprathermal outflows: the cleft ion fountain, the nightside auroral fountain (X-events, toroids and field-aligned flows) and polar cap outflows. The main emphasis is placed on flows at energies below about 50eV, observed by the Retarding Ion Mass Spectrometer (RIMS) on board the Dynamics Explorer 1 satellite; limited comparisons are made with results from other instruments which sample different energy ranges.

### INTRODUCTION

The injection of ionospheric ions into the magnetosphere has been a subject of keen interest since the discovery of  $O^+$  ions within the magnetosphere by Shelley et al /1/. Subsequently, other heavy ion species, known to be of ionospheric origin because of their virtual absence from the solar wind, have been revealed by mass-resolving ion spectrometers:  $N^+$  /2/,  $O_2^+$ ,  $NO^+$  and  $N_2^+$  /3/. Prior to these discoveries, the only known ionospheric ion outflow was the "polar wind", predicted by Banks and Holzer /4/ to comprise only the lighter ions,  $H^+$  and  $He^+$ . In addition, this "classical", steady-state polar wind was predicted to consist of ions of energy below about 1eV and to have maximum, "limiting" fluxes of order  $10^8 \text{ cm}^{-2} \text{ s}^{-1}$  (all outflux magnitudes quoted in this paper are normalised to a reference altitude of 1000 Km). Hence observations in the topside auroral ionosphere of suprathermal ionospheric ions /5, 6/ and steady-state outflows exceeding  $10^9 \text{ cm}^{-2} \text{ s}^{-1}$  /7, 8/ indicated that additional mechanisms operate which allow heavy ions to overcome the gravitational and charge exchange barriers and hence to escape from the ionosphere into the magnetosphere /9, 10/.

The Dynamics Explorer (DE) satellites have provided much new information on heavy and suprathermal ion additions to the classical polar wind. This review outlines the revolution in our knowledge of these ion flows which has been brought about by the DE mission.

### INSTRUMENTATION

The Dynamics Explorer mission comprised two spacecraft in coplanar polar orbits: DE1 covered a range of geocentric distances,  $r$ , up to spacecraft apogee of  $4.65R_E$ ; DE2 remained within the topside ionosphere at altitudes between 309 and 1012 km. The observations presented here were mainly made during the first 18 months of the mission from October 1981 to March 1983, during which DE1 apogee precessed from the north to the south polar cap and the plane of the orbits rotated through roughly 36 hours of magnetic local time. It is important to note that this period falls within the declining phase of the last solar cycle, shortly after sunspot maximum.

In this review, particular attention is paid to ions which are not greatly elevated in energy above the classical polar wind. Such ions are observed by the Retarding Ion Mass Spectrometer (RIMS) of the high-altitude DE1 satellite /11/. This experiment comprises three detector heads, the +Z, -Z and radial heads, aligned respectively, parallel, antiparallel and perpendicular to the satellite spin axis. The Z heads observe a broad acceptance cone around the perpendicular to the geomagnetic field and the radial head covers nearly a full range of pitch angles twice in every spin period of 6 seconds. Each head consists of a Retarding Potential Analyser, using retarding potentials in the range 0-50V, from whence ions enter an ion mass spectrometer giving mass-per-charge analysis over the range 1-32 amu/e. The energy range observed by RIMS varies with ion species.

For example, the 0-50V sweep of the RPA results in the observation of  $H^+$  ions of energy 0-175eV, where energy is measured relative to spacecraft potential,  $\phi_s$ : the corresponding values for  $He^+$  and  $O^+$  are 0-87eV and 0-57eV respectively. As  $\phi_s$  can be several volts positive when the ambient plasma density is very low, it is then necessary to apply a negative aperture bias (of magnitude exceeding  $\phi_s$ ) in order to observe the lowest energy plasma ( $<\phi_s$ eV). In general, RIMS was operated without such a potential bias but some observations made in bias mode are discussed in the next section.

In this paper only a limited attempt will be made to compare and contrast the observations made by RIMS with those from complimentary plasma experiments on both DE1 and DE2. Ions in the energy range 10eV-17 keV (again relative to  $\phi_s$ ) are observed by the Energetic Ion Composition Spectrometer (EICS) on DE1 /12/. High pitch angle and energy resolution observations of both ions and electrons were made by the High Altitude Plasma Instrument (HAPI) on DE1 /13/, the ion observations covering the range  $(5+\phi_s)$ eV to 13 keV but without mass resolution. Flows of thermal plasma in the topside ionosphere were observed by the Ion Drift Meter (IDM) on the low altitude DE2 spacecraft /14/. Together, these instruments have revealed the complexity of the mass coupling between the ionosphere and the magnetosphere and only recently has a coherent picture begun to emerge from their sometimes apparently contradictory findings.

#### THE "CLASSICAL" POLAR WIND

For many years the polar wind was a theoretical expectation, with only indirect evidence for its presence in the existence of the light ion trough and the latitudinal variation of the  $H^+$ - $O^+$  ion transition height /15, 16/. At low altitudes, collisions are very important and a hydromagnetic formulation, as employed by Banks and Holzer, is appropriate. However at great altitudes the flow will become collisionless and a kinetic formulation is required /17, 18/, the general case of evolution from hydrodynamic to kinetic regimes is a very difficult theoretical problem. A review of polar wind theories has been given by Raitt and Schunk /19/ and Moore /10/.

The classical polar wind is driven by a simple ambipolar electric field resulting from the spatial separation of free electrons and gravitationally-bound  $O^+$  ions. Light ions are continuously accelerated upward by this field at all latitudes at which the magnetosphere is unable to exert sufficient partial pressures to prevent the outflow. In practice the outflow is therefore expected everywhere outside the nightside, inner plasmasphere. For typical ionospheric densities and temperatures this leads to a steady-state outflow of mainly  $H^+$  ions with a maximum "limiting" flux set by the Coulomb drag between the  $H^+$  and the  $O^+$  ions. The escape of  $H^+$  ions is always subject to this limit because they are formed at low altitudes by charge exchange of geocoronal H atoms with  $O^+$  ions. This picture of the polar wind, driven only by the normal densities and temperatures of ionospheric plasma, leads to the following predictions:

- (a) The outflow is primarily  $H^+$  with only a few percent  $He^+$
- (b)  $O^+$  and other heavy ion species are gravitationally bound
- (c) flow velocities increase with altitude, becoming supersonic at a lower altitude for  $H^+$  than for  $He^+$
- (d) ion temperatures remain below  $\sim 8000K$  (ion energies  $< 1eV$ )
- (e) The outflow magnitude is of order  $10^8 \text{ cm}^{-2} \text{ s}^{-1}$ , the value limited by the H and  $O^+$  densities, the electron and ion temperatures, and the field-perpendicular drift velocity.

A steady-state outflow which obeys conditions (a) - (e) is referred to here as being the "classical" polar wind.

Observations of the classical polar wind are still surprisingly rare. Hoffman /20/ reported upward fluxes of  $H^+$  from Explorer 31 data and Hoffman and Dodson /21/ performed a statistical survey using the roll modulation of ion mass spectrometer data from ISIS 2. The flows in these studies were deduced by assuming the  $O^+$  was stationary, which may be the cause of the flux values being slightly smaller than predicted for the classical polar wind and of suprathermal flows being overlooked /8/. However, the observations indicated the limiting nature of the flux (by having a constant value independent of the ionospheric density fluctuations) and also showed that the flux persisted on closed sub-auroral and outer plasmaspheric field lines. At the altitude of ISIS 2 (1400 km), the flows were subsonic ( $1-5$  and  $1-3 \text{ Kms}^{-1}$  for  $H^+$  and  $He^+$  respectively). The supersonic nature of the polar wind at greater altitude was demonstrated using the RIMS experiment on DE1 in bias mode by Chappell et al /22/ and Sojka et al /23/. However accurate determination of supersonic polar wind parameters is hampered by lack of knowledge of the spacecraft

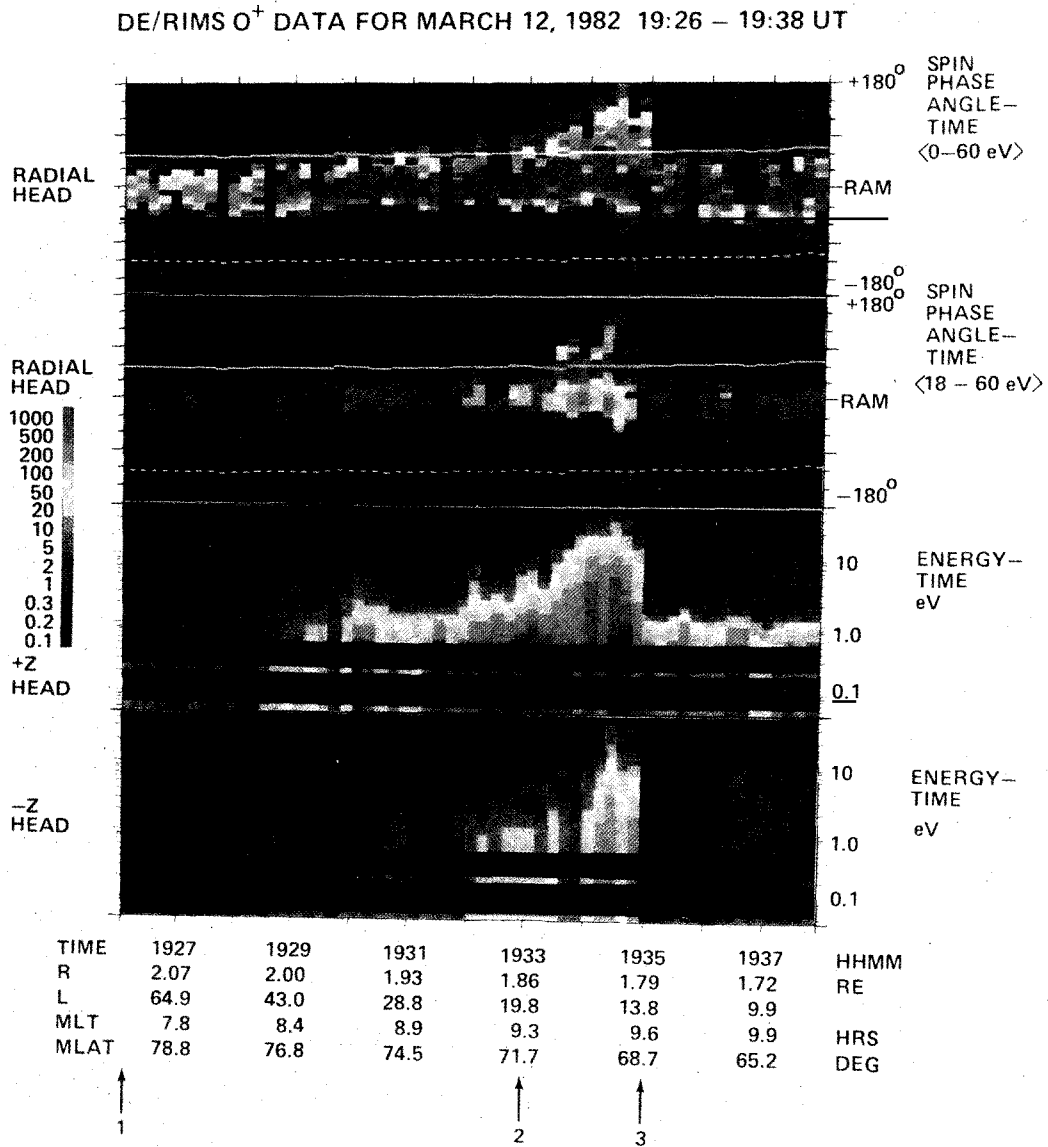


Fig. 1. Spin angle-time spectrograms from RIMS showing an example of an upwelling ion event. Transversely warmed ions are observed by the radial head at energies above 18eV (second panel) and by the Z heads (third and fourth panels) in the main part of the event (between the UT labelled 2 and 3).

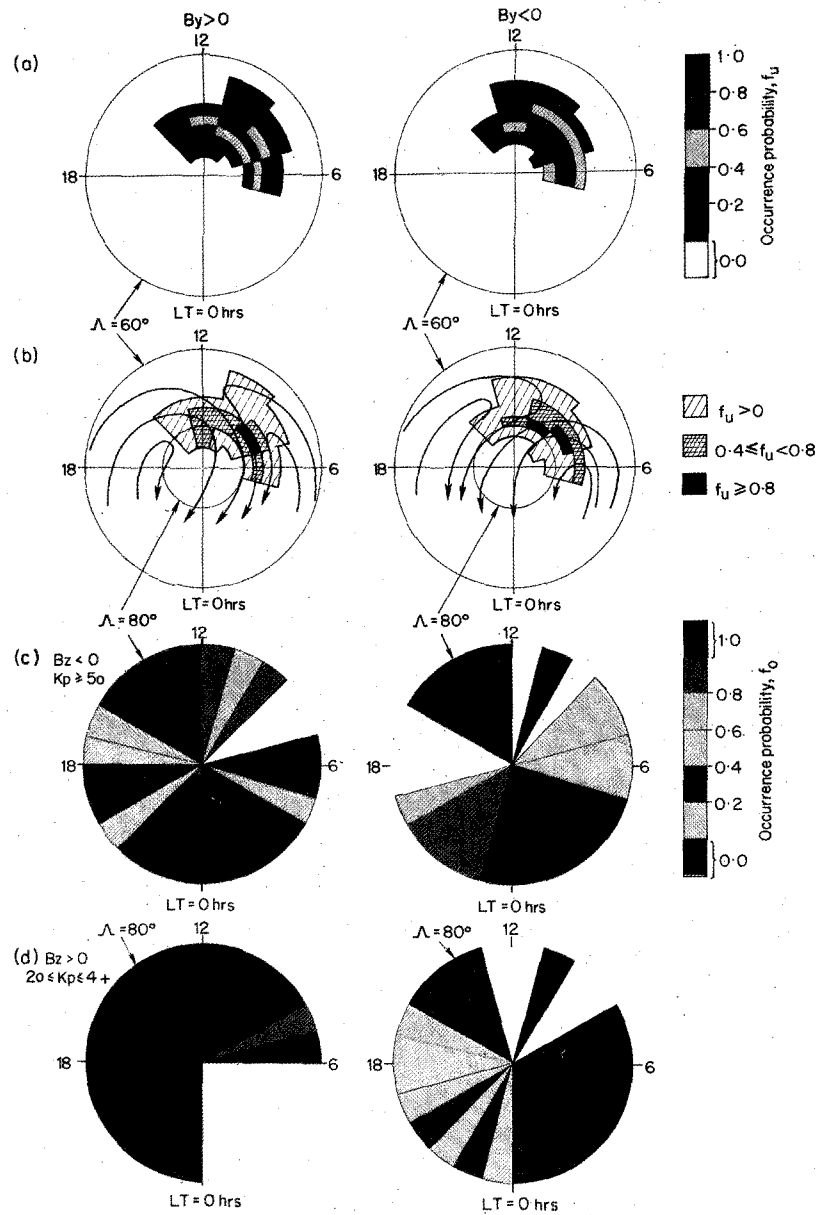


Fig. 6. The occurrence probability of upwelling ion  $O^+$  events,  $f_u$ , and of field-aligned  $O^+$  flows in the polar cap,  $f_o$ , for stable positive IMF  $B_y$  (left) and stable negative  $B_y$  (right). The top 2 panels show  $f_u$ ; (b) has typical convection patterns superposed. The lower 2 panels show  $f_o$  at  $\Lambda > 80^\circ$  for (c) IMF  $B_z < 0$  and  $K_p \geq 5$  and (d)  $B_z > 0$  and  $2.0 \leq K_p < 4+$ . The sense of the dawn-dusk asymmetries in  $f_o$  can be seen to depend on  $B_y$ , as predicted by the convection patterns and the cleft ion fountain.

potential,  $\phi_S$ . Nagai et al /24/ were able to define  $\phi_S$  for a period of bias-mode RIMS observations as being in the range 3-5V. Table 1 gives the plasma parameters derived from model fits using  $\phi_S$  in this range.

**TABLE 1** Polar Wind H<sup>+</sup> Parameters Observed by Nagai et al (1984)

| Spacecraft Potential<br>$\phi_S$ (V) | Temperature<br>(eV) | Velocity<br>(kms <sup>-1</sup> ) | Mach. No.<br>M | Ionospheric Outflux<br>(cm <sup>-2</sup> s <sup>-1</sup> ) |
|--------------------------------------|---------------------|----------------------------------|----------------|--|
| +3                                   | 0.2                 | 16                               | 2.6            | 1.6 x 10 <sup>8</sup>                                      |
| +4                                   | 0.15                | 21                               | 3.9            | 2.6 x 10 <sup>8</sup>                                      |
| +5                                   | 0.12                | 25                               | 5.1            | 2.6 x 10 <sup>8</sup>                                      |

These observations were in the nightside polar cap ( $\Lambda = 65-81^\circ$ ; MLT = 22:30-23:30) at  $r$  near  $3R_E$ . They are completely consistent with the classical polar wind, but the variability of the H<sup>+</sup>/He<sup>+</sup> ratio is surprisingly large.

Because it is expected to act over such a large area of the Earth, the classical polar wind is almost certainly the dominant ion outflow from the ionosphere into the magnetosphere (see review by Chappell et al /25/). Hence routine observations with full solution of the spacecraft potential problem are urgently required. In the meanwhile, we have to assume that the few available observations are typical and that constant, limiting outflow does indeed exist continuously everywhere outside the inner plasmasphere. Note that the area factor makes the polar wind on closed field lines a much greater source of magnetospheric plasma than that on open field lines.

#### SUPRATHERMAL ION OUTFLOWS

During the observations of the classical polar wind by Nagai et al the aperture bias applied to RIMS was cycled on and off. When no bias was applied, no ion flows were observed. This demonstrates that for this case (at  $r \approx 3R_E$ ) the spacecraft potential,  $\phi_S$ , was sufficiently large (3-5V) to prevent the observation of the classical polar wind without the application of the bias. In the remaining parts of this paper no bias-mode RIMS data will be discussed. Consequently, the observations at great altitudes will be of suprathermal ions of energy greater than  $\phi_S eV$ ; as a rough rule of thumb, the classical polar wind will only be observed at  $r < 2R_E$ , where  $\phi_S < 0$ .

The existence of suprathermal ionospheric ions within the magnetosphere was well known before DE mission (see reviews by Prange /26/ and Johnson /27/). Upward flows of both H<sup>+</sup> and O<sup>+</sup>, with energies exceeding 0.5 keV, were observed by the ion mass spectrometer on board the S3-3 satellite. Such ions display both conical and field-aligned pitch angle distributions and are most frequently found near the auroral oval /28, 29/. The auroral oval was found to be the source of ionospheric ions (of unknown mass) of energy greater than 90eV from a statistical survey of data from the electrostatic analyser on S3-3 /30/. In addition, the initial results from the EICS instrument on DE1 revealed that O<sup>+</sup> could be the dominant ion flow in the high altitude polar cap /31/ with most of the flux being observed in the lowest EICS energy channel ( $< \phi_S + 125eV$ ). The occurrence frequency of such flows has been studied by Yau et al /32/ and found to be as great as 0.3 (for the energy range  $(\phi_S + 10)eV - 1keV$ ). The RIMS instrument also found strong fluxes of O<sup>+</sup> in the polar cap between 2 and 4  $R_E$  when Kp was high /33/. The importance of these observations by Waite et al. lies in their recognition of the implications of the low energies (2-8eV) of the O<sup>+</sup> ions seen by RIMS: the consequent large times of flight from the ionosphere and the antisolar convection drifts (observed by the IDM on DE2) locate the sources of these ions considerably sunward of the points of observation. This concept was also used by Green and Waite /34/ to point out that an apparently suprathermal polar wind component in the polar cap /35/ was in fact O<sup>+</sup> ion flows convected from a spatially-displaced source region.

#### Upwelling Ion Events

The observations by Waite et al /33/ called for a source of cold O<sup>+</sup> ions at low altitudes near the dayside auroral oval. A statistical survey of the first 18 month's data from RIMS by Lockwood et al /36/ identified the cleft to be just such a source. This is the

most persistent suprathermal outflow feature observed by RIMS and the ion flows have been termed upwelling ions because all observed species ( $H^+$ ,  $He^+$ ,  $O^+$ ,  $O^{++}$  and  $N^+$ ) are warmed, flowing upward and carrying an upward heat flux. Craven et al /3/ have shown that even molecular ions  $N_2^+$ ,  $O_2^+$  and  $NO^+$  can be injected into the magnetosphere in the upwelling ion region. Moore et al /37/ have presented a detailed study of an upwelling ion event which is summarised in Figures 1 and 2. The events carry large fluxes of ions ( $H^+$  and  $O^+$  fluxes out of the ionosphere of order  $10^9 \text{ cm}^{-2} \text{ s}^{-1}$ ), as deduced from Figure 2d. Note that equatorward of the event, the classical polar wind fluxes of  $H^+$  and  $He^+$  can be seen (after the UT labelled 3), but not poleward of it (before the UT labelled 1). As there is no reason to suspect the polar wind to be absent from these polar cap field lines, we conclude that the geocentric distance  $r$ , and resulting spacecraft potential  $\phi_s$ , must be too great to allow observation of the classical polar wind before 1. Likewise near-thermal  $O^+$  ( $< \phi_s \text{ eV}$ ) would not be observed before 1 and total outflux estimates are hence absolute minima as they take no account of this hidden, lowest-energy component. Part (c) of Figure 2 illustrates that the sharp equatorward edge of these events is closely associated with that of field-aligned current regions; the two migrate equatorward together at times of high  $K_p$  /36/. The equatorward edge of the event is also associated with a strong eastward convection channel /37/ where the event also shows the effects of transverse ion heating (Figure 2b) with a near-bimaxwellian distribution function (which evolves into folded conical lobes and rammed field aligned flow as the ions convect poleward).

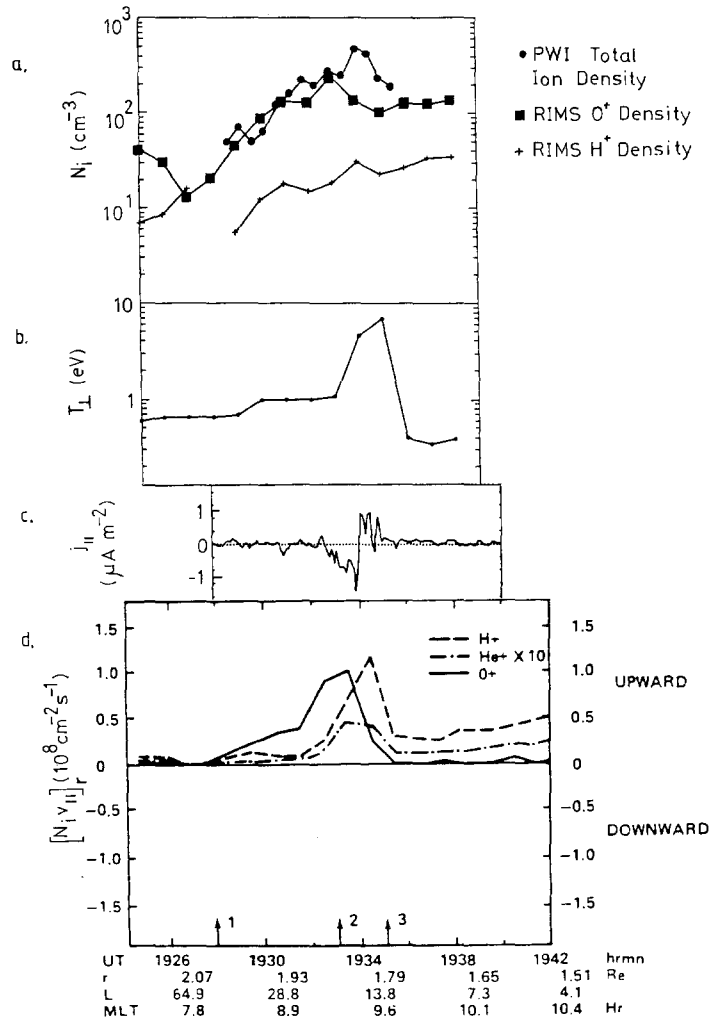


Fig. 2. Characteristics of the upwelling ion event shown in Figure 1. (a) The ion densities,  $N_i$ , observed by RIMS, contrasted with the total ion density from the DE1 Plasma Wave Instrument. (b) The transverse  $O^+$  ion temperature,  $T_{\perp}$ , from the  $-Z$  head of RIMS. (c) The inferred field-aligned current,  $j_{\parallel}$ , from the DE1 magnetometer. (d) The field-aligned fluxes of  $O^+$ ,  $H^+$  and  $He^+$ ,  $N_i v_{\parallel}$ , computed for the altitude of DE1 from the RIMS radial head data. The UT labelled 1, 2 and 3 are as for Figure 1.

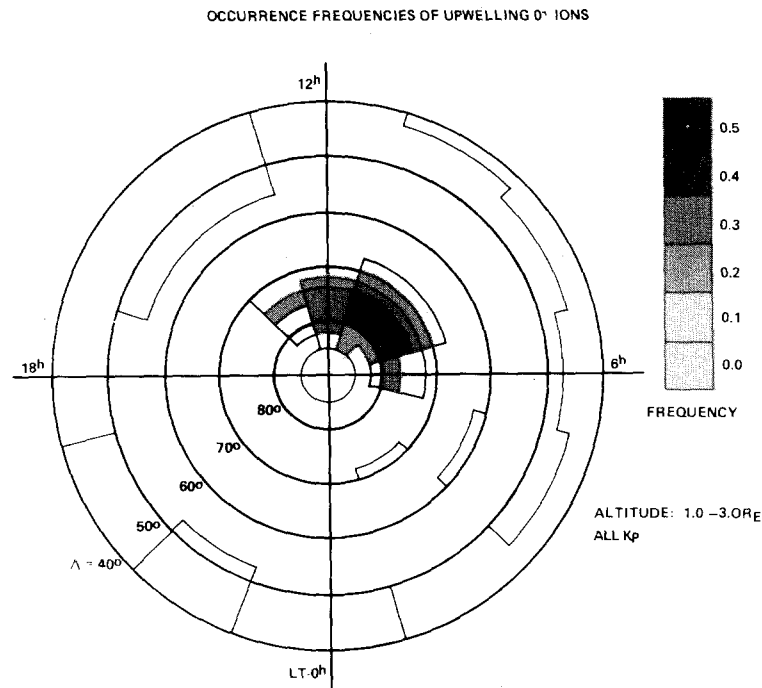


Fig. 3. The occurrence probability of upwelling O<sup>+</sup> ion events as a function of MLT and invariant latitude,  $f_u$ . These data are for geocentric distances,  $r$ , of 1-3  $R_E$ , all Kp and the first 18 months of the DE mission (sunspot maximum) (from /36/).

Figure 3 shows the occurrence frequency of upwelling O<sup>+</sup> ion events for  $r < 3R_E$  /36/. It can be seen that this can exceed 0.6 per invariant latitude-MLT bin, and integrated along an MLT meridian in the pre-noon sector it is unity. That upwelling cleft ion events are virtually always present in the cleft is now being confirmed by the particle spectrometers on the VIKING satellite (Lundin, private communication). However, it is not clear that they are so persistently strong in O<sup>+</sup> in the VIKING data, which is for sunspot minimum. Hence there is an indication of a solar cycle variation in the O<sup>+</sup> content of upwelling ion events.

The importance of these flows to the composition of the inner polar magnetosphere is demonstrated by Figure 2a. It is shown that the density of O<sup>+</sup> ions observed by RIMS (ie energies of  $\phi_S - (\phi_S + 60)eV$ ) is virtually equal to the total plasma density observed by the Plasma Wave Instrument (PWI) on DE1. Hence the plasma is dominated by upwelling O<sup>+</sup> ions.

#### The Geomagnetic Mass Spectrometer

From the narrow nature of the upwelling ion source region, Lockwood et al /36/ concluded that ions should be spatially dispersed across the polar cap according to their time of flight. For a given ion species, lower energy ions will be convected further toward the nightside, as will heavier ions for a given ion energy. Waite et al. /33/ had observed the energy dispersion of the O<sup>+</sup> ions within the polar cap to extend continuously from several keV (observed by EICS near the cleft) to several eV (observed by RIMS in the nightside polar cap) (see also /40/). The mass dispersion of upgoing ionospheric ions of the same energy had been noted by Moore et al /38/ who termed the effect the "geomagnetic mass spectrometer". First-order quantification of the effect was made possible by a two-dimensional kinetic trajectory model by Horwitz /39/. Note that these observations do not necessarily imply that the ions of different species are energized to similar energies in upwelling ion events; that RIMS observes mass dispersion may be entirely due to the fact that it only samples a limited energy range. Lockwood et al /40/ have found that O<sup>+</sup> ions are heated up to a maximum of about 2 keV and other EICS-RIMS comparisons are revealing this is a hot tail to a warmed O<sup>+</sup> distribution. It is difficult to evaluate the limit of H<sup>+</sup> heating as heated ionospheric H<sup>+</sup> cannot be distinguished from the injected and mirrored solar wind H<sup>+</sup>. However, it appears that an approximate range of 0-2keV may also be applicable to H<sup>+</sup>. If confirmed, this has great implications for the identification of the heating processes which are responsible for upwelling ion events.

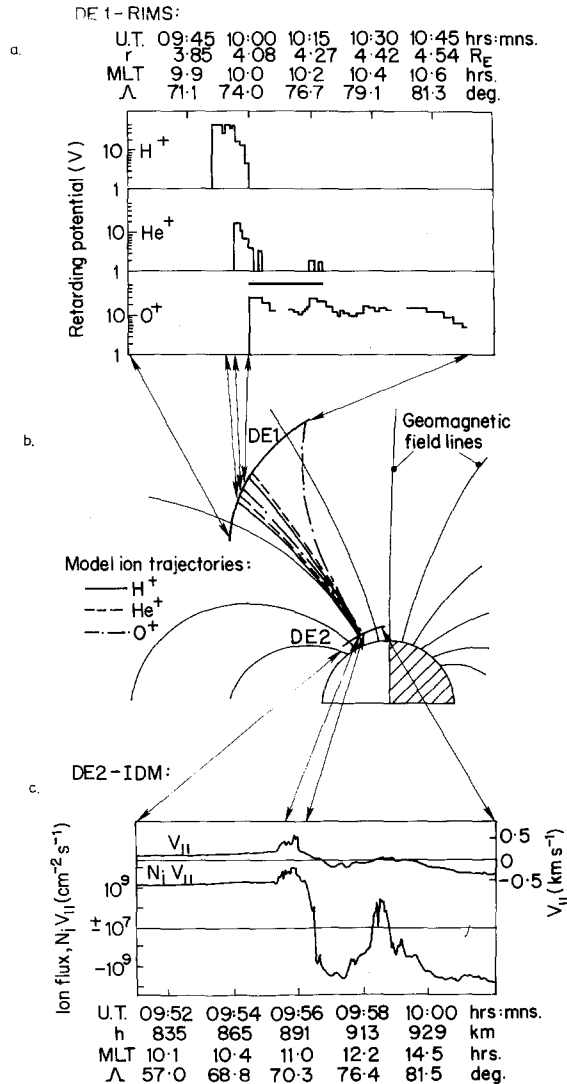


Fig. 4. The geomagnetic mass spectrometer. (a) the retarding voltages to reduce the  $H^+$ ,  $He^+$  and  $O^+$  count rates to the noise level, observed by DE1-RIMS, equivalent to the peak ion energies. (b) 2-dimensional ion trajectories computed for the ions observed by RIMS using antisunward convection component observed by DE2. (c) Field-aligned velocity,  $v_{||}$ , and flux,  $N_i v_{||}$ , observed in the same period by DE2. All ions seen by DE1 map back to a narrow source region in the cleft topside ionosphere where DE2 observed a large upflux. (from /41/).

Figure 4 shows a conjunction between DE1 and DE2 which illustrates the mass spectrometer effect on ions observed by RIMS in the high altitude polar cap (Figure 4a) /41/. In part b of Figure 4, the ion trajectories are traced Earthward from DE1 using the convection velocity observed by the IDM on DE2 and the trajectory model by Horwitz /39/. The trajectory computations employ a simple allowance for the ambipolar parallel electric field and assume a free, test particle approach. As such, they are obviously simplistic but to date no more rigorous computations have been made. They indicate that all the ions observed by RIMS originated from a narrow source in the topside ionosphere where indeed the IDM on DE2 observed strong thermal plasma outflow ( $> 10^9\ cm^{-2}\ s^{-1}$ ). These outfluxes have been confirmed by statistical studies using the HILAT satellite /42/ and have similar occurrence to that of upwelling ion events. Note that poleward of this upflux, flows in the low-altitude polar cap are generally downward, a feature also noted in AUREOL-3 data /43, 44, 45/.

Comparison of total ion and cold  $O^+$  densities, as presented for the mid-altitude dayside cap ( $r \approx 2R_E$ ), in Figure 2a, show that  $O^+$  ions also dominate for the pass of DE1 depicted in Figure 4, i.e. even in the high altitude ( $r \approx 4R_E$ ) dayside polar cap /40/.

**The Cleft Ion Fountain**

The analogy of the geomagnetic ion mass spectrometer does not allow for the effect of gravity which remains a significant factor in the motion of low-energy ionospheric ions. Predicted trajectories show that the lowest energy heavy upwelling ions would fall Earthward under gravity in the polar cap /39/. Lockwood et al. /46/ observed  $O^+$ ,  $N^+$ ,  $O^{++}$  and even  $He^+$  flowing downward at low altitudes in the cap. With the assumption that the  $O^+$  and  $O^{++}$  originate from the same source region, the relative motion of these two ion species, which differ only in their charge states, can be used to estimate the ambipolar field-aligned electric field. The value ( $\sim 0.1 \mu Vm^{-1}$  in the topside ionosphere) is consistent with the predictions of the classical polar wind but is inconsistent with observations of photoelectron energies by Winningham and Gurgiolo /47/: the total potential drop they determined is 1 to 2 orders of magnitude greater but may be at greater altitudes. Lockwood et al /46/ have shown that even for these larger fields, heavy ionospheric ions should fall downward in the cap. Hence to allow for the effect of gravity, these authors introduced the "fountain in a wind" analogy and termed the outflow the "cleft ion fountain". The downflows seen in the topside polar cap ionosphere would then be the lowest energy component of the fountain. Berthelier /45/ has shown that these downflows are consistent with convection of plasma through the cleft and the transient response of the convecting flux tube to particle precipitation. The resulting upwelling of thermal plasma in the cleft would supply cold ions which could be heated to give suprathermal upwelling ions and the cleft ion fountain; the convection of ionospheric plasma into the cleft ensures that this supply is both plentiful and continuous.

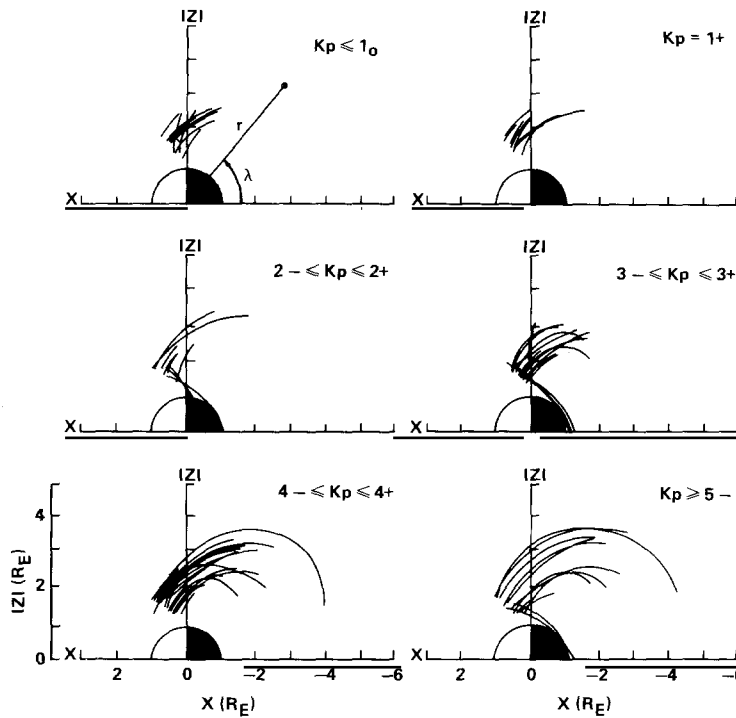


Fig. 5. Locations, for various Kp ranges, where DE1-RIMS observed polar cap  $O^+$  contiguous with upwelling ion events /46/. RIMS will observe  $O^+$  when the density of ions of energy  $\phi_s$  to 60 eV exceeds about  $1cm^{-3}$ . The  $O^+$  can be seen to be swept further across the cap at higher Kp values.

The role of convection in filling the polar cap with  $O^+$  from the cleft ion fountain is demonstrated by Figures 5 and 6. Figure 5 shows segments of DE1 orbits where RIMS observes  $O^+$  ions in the polar cap contiguous with upwelling ion events /46/. The data are binned into six Kp ranges. For low Kp, the  $O^+$  is only found on the dayside; however for Kp greater than about 4 the  $O^+$  extends throughout the cap, consistent with the variation at occurrence probability of  $O^+$  in the polar cap with Kp found by Waite et al /33/. The spreading for the  $O^+$  has been modelled by Horwitz and Lockwood /48/. The results of Kp  $\sim 1$  were found to be consistent with a convection electric field strength in the ionosphere of  $20mV m^{-1}$ ; for Kp>5 a value of roughly  $80mV m^{-1}$  is required. The high occurrence probabilities of  $O^+$  in the cap for Kp>5 are underlined by Figure 6. The data have been

sorted according to the sense of  $B_y$  and are for cases where the IMF is stable for a 3-hour period prior to, and including, the time of the RIMS observation. The third panel of Figure 6 shows the occurrence probability of  $O^+$  flow,  $f_0$ , at  $\Lambda > 80^\circ$  as a function of MLT, for southward IMF ( $B_z < 0$ ) and  $K_p > 5$ . The red areas have a probability of exactly unity. It can be seen that there is a strong dawn-dusk asymmetry in the  $O^+$  flows, dependent on the sense of  $B_y$ . For  $B_y > 0$ ,  $f_0$  is unity or near unity on the dawnside only; for  $B_y < 0$ , the flows fill a larger portion of the cap, but  $f_0$  is lowest near dawn. The top panels show the occurrence probability of upwelling ion events,  $f_u$ , for the same  $B_y$  bins, overlaid with convection trajectories, typical of the two  $B_y$  senses, from the work of Heelis /49/. It can be seen that there is no clear  $B_y$  effect on the location of the upwelling ions and hence the effect on the polar cap  $O^+$  flow morphology must be due to the differences between the convection patterns. The bottom panel of Figure 6 demonstrates that the same  $B_y$  asymmetry is found for the available northward IMF data ( $B_z > 0$ ), but  $f_0$  values tend to be lower for a larger part of the cap, presumably due to a region of sunward convection /50/. Figure 7 shows the occurrence frequency,  $f_0$ , of field-aligned flows of  $O^+$  and  $H^+$  observed by RIMS in the high altitude polar cap during disturbed conditions. Plots of  $f_0$  as a function of invariant latitude are shown for various ranges of  $r$  with the dayside to the left of the figure and the nightside to the right. The  $O^+$  flows are nearly always present ( $f_0=1$ ) at all  $r$  in the dayside cap, whereas  $f_0$  is near zero throughout most of the cap for  $H^+$ . It must be remembered that these observations are of ions of energy greater than  $\phi_S$  eV, and that  $\phi_S$  is almost certainly positive at these  $r$ ; hence classical polar wind ions are excluded. The ions in the cap are mainly of energy below 10 eV /33, 40/ and all map back to the cleft ion fountain source. Hence, according to the geomagnetic spectrometer dispersion principle, the fall in  $f_0$  at  $\Lambda < 80^\circ$  on the nightside would then be due to the ion energy falling below  $\phi_S$ , which would occur at greater  $\Lambda$  for greater  $r$  where  $\phi_S$  is larger. Hence lower energy ( $< \phi_S$ ), hidden  $O^+$  is to be expected in the lower latitudes of the nightside polar cap and should feed into the nightside oval when convection is sufficiently strong.

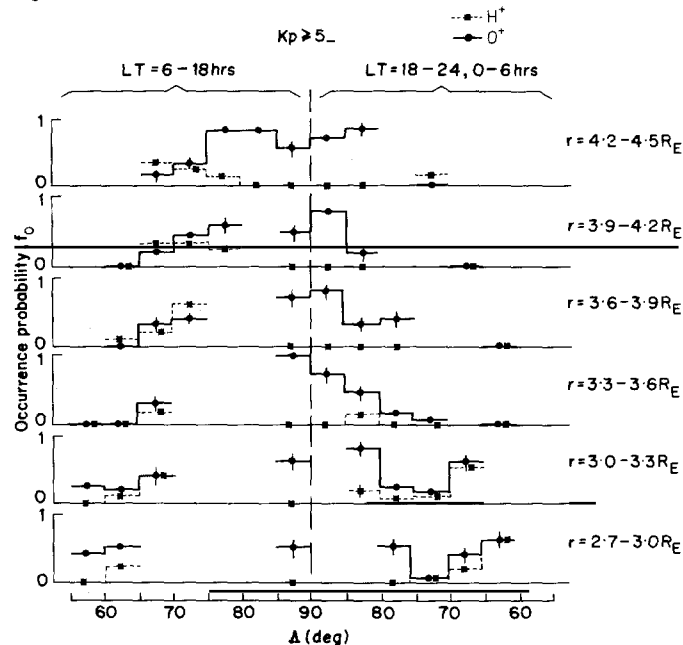


Fig. 7. The occurrence probability of field-aligned upflows of  $O^+$  and  $H^+$ ,  $f_0$ , seen by RIMS in various ranges of geocentric distance,  $r$ . Values are given only where more than 20 samples are available, and are shown as a function of invariant latitude,  $\Lambda$ , for the dayside (left) and the nightside (right).

### Nightside X-Events

Moore et al. /38/ have described occurrences of ion conics sandwiching an upgoing beam in the nightside auroral oval, the continuous folding of the conics into the beam giving an X-shaped form to the RIMS spin angle-time spectrograms for all ion species. These events are found near shear-like polar cap boundary reversals and are associated with inverted-V electron precipitation structures. They would give rise to higher altitude fluxes which were mainly on closed, auroral nightside field lines and would be included in the auroral zone fluxes computed from EICS data by Yau et al. /32, 51/. The occurrence frequency of these events is not well known but they are comparatively rare. One of these events is discussed in greater detail by Lockwood et al /52/.

### Nightside Toroidal Distributions

Moore et al /38/ and Lockwood et al /36/ have reported a form of low-energy ion upflows which are exotic in that they result from coherent transverse acceleration, giving a toroidal form to the distribution function, /53/. These distributions have been found for all observed species ( $O^+$ ,  $H^+$ ,  $He^+$ ,  $N^+$  and  $O^{++}$ ). The rates at which the pitch angle peaks fold are mass dependent as is the apparent altitude of the heating /54/. Although the occurrence frequency is lower ( $\sim 0.2$  in the nightside oval /36/) these events cover a wide range of invariant latitudes. The total ion flux which they carry is not yet known but convection will result in them supplying ions to both auroral and sub-auroral closed, nightside field lines.

### Other Auroral Flows

The statistical surveys of topside ion flows by Klumpar /6/ and Lockwood /8/ showed that most of the auroral oval should act as a source of suprathermal plasma. This is consistent with the high altitude distribution of energetic ( $>90$ eV) beams and conics and the surveys of EICS data by Yau et al /32, 51/.

In addition to the "X" and toroidal outflows discussed in the previous two sections, RIMS should observe "hot-tail" conics which, unlike toroidal distributions, do not have a heated core to the distribution function. These ions would have originated as "Transversely Accelerated Ions" in the topside ionosphere /6/ but may be difficult to observe with RIMS as they will tend to be masked in spin angle-time spectrograms by the unheated core of the distribution.

Figure 7 shows some upward field-aligned flows in the nightside auroral oval ( $70^\circ < \lambda < 60^\circ$ ) at lower altitudes ( $r < 3.3R_E$ ). At greater  $r$  the data are very sparse, but where they do exist RIMS sees no flows. Upward flows are frequently observed in this region by EICS /32, 51/; hence they must be at energies above the upper limit of RIMS, suggesting that secondly acceleration mechanisms are operating at the greater altitudes.

### COMPARISONS WITH OTHER DATA ON $O^+$ ION OUTFLOWS

Time-of-flight and convection effects are greatest for low-energy, heavy ion outflows. The most widely studied of these species has been  $O^+$  (although it should be noted that  $N^+$  often shows very similar behaviour to  $O^+$  when both are observed /46/). In this section the variations in  $O^+$  flow morphology with energy are discussed.

The occurrence frequency of  $O^+$ , seen within the polar cap by EICS, is lower than for the auroral oval, but still as large as 0.3 /32/. Yau et al /51/ have estimated that the total flux in the mid-altitude polar cap is 10-25% of the total outflow (polar cap and auroral) at low  $K_p$ , rising to 20-35% at moderately high  $K_p$ . These flows are at energies above  $(10 + \phi_S)$ eV and Yau et al have found that 90% of this flux was at energies below 1keV. However, the  $O^+$  flux in the cap observed by RIMS is nearly all at energies below  $(\phi_S + 10)$ eV /33, 40/ and hence would not have been observed by EICS. An accurate assessment of the extra flux at energies between  $\phi_S$  and  $(\phi_S + 10)$ eV from RIMS is made difficult by the requirement that the convection electric field at DE1 be accurately known.

The flows seen by RIMS certainly map back to a cleft ion fountain source, but simple trajectories for much of the  $O^+$  observed by EICS indicates the energies are too great for this to be true in their case /31/. This would require that either there is a source within the polar cap, perhaps driven by polar rain or joule heating (unlikely in view of the downward flows seen throughout the cap in the topside ionosphere) or that the cleft ion fountain ions undergo secondary acceleration at high altitudes within the cap. A recent paper by Cladis /55/ may go a long way in resolving this question. In moving upward along curved and tilted geomagnetic field lines, the ions will undergo a form of "slingshot" acceleration. This effect is certainly important at greater altitudes and shows that cleft fountain  $O^+$  ions will reach lower plasma sheet energies as a natural consequence of their transport. In this case, the strong  $K_p$  dependence of upwelling ions /36/ would be the principal modulator of plasma sheet composition /56/. Likewise any solar cycle variation in the  $O^+$  content of upwelling ions could explain the solar cycle dependence of plasma sheet  $O^+$ . The  $O^+$  flows observed by EICS also show both the required  $K_p$  and solar cycle dependences /51/. Note that the  $O^+$  ions continuously gain energy along their paths, hence the boundary of the plasma sheet will appear at different locations to  $O^+$  detectors with differing low energy thresholds.

Without observations down to 0eV, it is not possible to tell what flux of  $O^+$  ions is fed across the polar cap into the nightside auroral oval by the cleft ion fountain. Hence the balance between the cleft ion fountain ionospheric ion source and the nightside auroral ionosphere is not accurately known. In theory, the cleft ion fountain can inject its

highest energy heavy ions into the plasma sheet via the lobes and its lowest energy heavy ions into the nightside acceleration regions to give upward flowing ions of the kind discussed by e.g. Collin et al /29/ and Yau et al /32/. Lockwood et al /36/ estimated the average total  $O^+$  outflux in the fountain to be at least  $10^{25} s^{-1}$ . This figure is inadequate for the cleft to be the ionospheric source of all  $O^+$  observed by EICS /51/ but is also an underestimate because of spacecraft potential effects: an approximate average figure of  $10^{26} s^{-1}$  arises from the cleft fountain flux seen by DE2 /41/. This compares with total  $O^+$  outflow magnitudes of under  $10^{25} s^{-1}$  for  $Kp < 1$  rising to over  $10^{26} s^{-1}$  for  $Kp > 5$  found by a much more thorough survey of EICS data by Yau et al /51/.

#### ION HEATING MECHANISMS RESPONSIBLE FOR SUPRATHERMAL IONOSPHERIC ION OUTFLOWS

The mechanisms which elevate ionospheric ions in energy, and hence altitude, could form the subject of a large review in their own right, so many, varied and complex are the processes which have been suggested. Here it is only possible to mention briefly some of those hinted at by observations by the DE satellites. Lockwood et al /40/ have found that transverse  $O^+$  heating is occurring on the equatorward edge of upwelling ion events, in a narrow region of intense upgoing ionospheric electron beams, observed by HAPI /57/. This suggests an electrostatic ion cyclotron resonance as described by Dusenbury and Lyons /58/. This would give  $O^+$  outflow in the manner described by Moore /9/ and Lockwood /59/. However, the intense  $O^+$  fluxes are found on field lines where DE2 observes exceptionally high (up to 14000K) electron temperatures, similar to those described by Curtis et al /60/. Barakat and Schunk /61/ have shown how such extreme electron temperatures can add suprathermal beams of  $O^+$  to the "classical" polar wind by simply increasing the ambipolar, charge separation electric field. The upwelling of thermal plasma in the cleft can explain the observed downward flows within the cap /45/ and Singh and Schunk /62/ have shown that such a transient expansion can also add suprathermal  $O^+$  to the outflow. As discussed in the previous section, convection into the cleft region can allow this transient phenomena to persist continuously. Ion heating by ion-neutral frictional heating, can also produce a similar continuous yet transient outflow /63/. At present, the relative importance of these various mechanisms is not clear.

On the nightside, the X-events are consistent with upward parallel acceleration by a field-aligned potential structure in the event centre, the transverse acceleration on the edges also arising from the potential structure /64/. The formation and stability of toroidal distributions has been discussed by Moore et al /53/. A recent review of possible heating mechanisms has been given by Moore /65/.

#### CONCLUDING REMARKS

The low-energy ion outflow observed by RIMS comprises a "classical" polar wind along with additional suprathermal and heavy ion flows. The classical polar wind is assumed to be relatively unvarying in time and space, but direct observational evidence of this constancy is not yet available. However, the suprathermal outflows, particularly of  $O^+$ , are known to be highly structured and to vary greatly with magnetic activity and solar activity. Time-of-flight and transport effects make the identification of ionospheric source regions very difficult. Recently, Chappell et al /25/ have made the first attempt to assess the relative importance of the cleft ion fountain, nightside auroral and polar cap suprathermal ion sources by combining RIMS and EICS findings. Of the three, the polar cap ionosphere appears to be the smallest by an order of magnitude; however in terms of the total ion outflow all three are at least an order of magnitude smaller than the classical polar wind, if indeed it is as spatially constant as is expected. The plasma composition of different parts of the magnetosphere will be determined by different ionospheric outflow mechanisms and in evaluating their contributions, allowance must be made for both time-of-flight velocity filter effects and slingshot ion acceleration.

#### REFERENCES

1. E.G. Shelley, R.G. Johnson and R.D. Sharp, Satellite observations of energetic heavy ions during a geomagnetic storm, J. Geophys. Res., 77, 6104 (1972).
2. C.R. Chappell, R.C. Olsen, J.L. Green, J.F.E. Johnson, and J.H. Waite, Jr., The discovery of nitrogen ions in the earth's magnetosphere. Geophys. Res. Lett., 9, 937 (1982).
3. P.D. Craven, R.C. Olsen, C.R. Chappell and L. Kakani, Observations of molecular ions in the earth's magnetosphere, J. Geophys. Res., 90, 7599 (1985).
4. P.M. Banks and T.E. Holzer, High-latitude plasma transport: The polar wind, J. Geophys. Res., 74, 6317 (1969).

5. B.A. Whalen, W. Bernstein and P.W. Daly, Low altitude acceleration of ionospheric ions, Geophys. Res. Lett., 5, 55 (1978).
6. D.M. Klumpar, Transversely accelerated ions: an ionospheric source of hot magnetospheric ions, J. Geophys. Res., 84, 4229 (1979).
7. M. Lockwood and J.E. Titheridge, Ionospheric origin of magnetospheric  $O^+$  ions, Geophys. Res. Lett., 8, 381 (1981).
8. M. Lockwood, Thermal ion flows in the topside auroral ionosphere and the effects of low-altitude, transverse acceleration, Planet. Space Sci., 30, 595 (1982).
9. T.E. Moore, Modulation of terrestrial escape flux composition (by low-altitude acceleration and charge exchange chemistry), J. Geophys. Res., 85, 2011 (1980).
10. T.E. Moore, Superthermal ionospheric outflows, Rev. Geophys., 22, 264 (1984).
11. C.R. Chappell, S.A. Fields, C.R. Baugher, J.H. Hoffman, W.B. Hanson, W.W. Wright and H.D. Hammack, The retarding ion mass spectrometer on Dynamics Explorer-A., Space Sci. Instrum., 5, 477 (1981).
12. E.G. Shelley, D.A. Simpson, T.C. Sanders, E. Hertzberg, H. Balsiger, A. Ghielmetti, The energetic ion composition spectrometer (EICS) for the Dynamics Explorer-A., Space Sci. Instrum., 5, 443 (1981).
13. J.L. Burch, J.D. Winningham, V.A. Blevins, N. Eaker, W.C. Gibson and R.A. Hoffman, High-altitude plasma instrument for Dynamics Explorer-A., Space Sci. Instrum., 5, 455 (1981).
14. R.A. Heelis, W.B. Hanson, C.R. Lippincott, D.R. Zuccaro, L.H. Harmon, B.J. Holt, J.E. Doherty and R.A. Power, The ion drift meter for Dynamics Explorer-B., Space Sci. Instrum., 5, 511 (1981).
15. W.J. Raitt and E.B. Dorling, The global morphology of light ions measured by the ESRO-4 satellite, J. Atmos. Terr. Phys., 38, 1077 (1976).
16. J.E. Titheridge, Ion transition heights from topside electron density profiles, Planet. Space Sci., 24, 229 (1976).
17. J. Lemaire and M. Scherer, Model of the polar ion-exosphere, Planet. Space Sci., 18, 103 (1970).
18. J. Lemaire and M. Scherer, Kinetic models of the solar and polar winds, Rev. Geophys. Space Phys., 11, 427 (1973).
19. W.J. Raitt and R.W. Schunk, Composition and characteristics of the polar wind, in: Energetic Ion Composition in the Earth's Magnetosphere, Terra Scientific Publishing Co., Tokyo (1983).
20. J.H. Hoffman, Studies of the composition of the ionosphere with a magnetic deflection mass spectrometer, Int. J. Mass Spectrom. Ion Phys., 4, 315 (1970).
21. J.H. Hoffman and W.H. Dodson, Light ion concentrations and fluxes in the polar regions during magnetically quiet times, J. Geophys. Res., 85, 626 (1980).
22. C.R. Chappell, J.L. Green, J.F.E. Johnson and J.H. Waite Jr., Pitch angle variations in the magnetospheric thermal plasma: initial observations from Dynamics Explorer-1, Geophys. Res. Lett., 9, 933 (1982).
23. J.J. Sojka, R.W. Schunk, J.F.E. Johnson, J.H. Waite Jr. and C.R. Chappell, Characteristics of the thermal and suprathermal ions associated with the dayside plasma trough as measured by the Dynamics Explorer Retarding Ion Mass Spectrometer, J. Geophys. Res., 88, 7895 (1983).
24. T. Nagai, J.H. Waite Jr., J.L. Green and C.R. Chappell, First measurements of supersonic polar wind in the polar magnetosphere, Geophys. Res. Lett., 11, 669 (1984).
25. C.R. Chappell, T.E. Moore and J.H. Waite, Jr., Is there any solar wind plasma in the Earth's magnetosphere? J. Geophys. Res., submitted (1986).

26. R. Prange, Energetic (keV) ions of ionospheric origin in the magnetosphere, A review. Annls Geophys. 34, 187 (1978).
27. R.G. Johnson, Energetic ion composition in the Earth's magnetosphere, Rev. Geophys. Space Phys., 17, 696 (1979).
28. A.G. Ghielmetti, R.G. Johnson, R.D. Sharp and E.G. Shelley, The latitudinal, diurnal and altitudinal distributions of upward flowing energetic ions of ionospheric origin, Geophys. Res. Lett., 5, 59 (1978).
29. H.L. Collin, R.D. Sharp and E.G. Shelley, The magnitude and composition of the outflow of energetic ions from the ionosphere, J. Geophys. Res., 89, 2185 (1984).
30. D.J. Gorney, A. Clarke, D. Croley, J. Fennell, J. Luhmann and P. Mizera, The distribution of ion beams and conics below 8000 km, J. Geophys. Res., 86, 83 (1981).
31. E.G. Shelley, W.K. Peterson, A.G. Ghielmetti and J. Geiss, The polar ionosphere as a source of energetic magnetospheric plasma. Geophys. Res. Lett., 9, 941 (1982).
32. A.W. Yau, B.A. Whalen, W.K. Peterson and E.G. Shelley, Distribution of upflowing ionospheric ions in the high-altitude polar cap and auroral ionosphere, J. Geophys. Res., 89, 5507 (1984).
33. J.H. Waite, Jr., T. Nagai, J.F.E. Johnson, C.R. Chappell, J.L. Burch, T.L. Killen, P.B. Hays, G.R. Carignan, W.K. Peterson and E.G. Shelley, Escape of suprathermal  $O^+$  ions in the polar cap, J. Geophys. Res., 90, 1619 (1985).
34. J.L. Green and J.H. Waite Jr., On the origin of polar ion streams, Geophys. Res. Lett. 12, 149 (1985).
35. C. Gurgiolo and J.L. Burch, DE-1 observations of the polar wind - A heated and an unheated component, Geophys. Res Lett., 9, 945 (1982).
36. M. Lockwood, J.H. Waite Jr., T.E. Moore, J.F.E. Johnson and C.R. Chappell, A new source of suprathermal  $O^+$  ions near the dayside polar cap boundary, J. Geophys. Res., 90, 4099 (1985).
37. T.E. Moore, M. Lockwood, M.O. Chandler, J.H. Waite, Jr., C.R. Chappell, A. Persoon and M. Sugiura, Upwelling  $O^+$  ion source characteristics, J. Geophys. Res., 91, 7019 (1986).
38. T.E. Moore, C.R. Chappell, M. Lockwood and J.H. Waite, Jr., Superthermal ion signatures of auroral acceleration processes, J. Geophys. Res., 90, 1611 (1985).
39. J.L. Horwitz, Features of ion trajectories in the polar magnetosphere, Geophys. Res. Lett., 11, 1111 (1984).
40. M. Lockwood, J.H. Waite, Jr., T.E. Moore, M.O. Chandler, C.R. Chappell, J.L. Horwitz, R.A. Heelis, M. Sugiura, W.K. Peterson, A. Persoon, J.L. Burch, C.S. Lin, J.D. Menietti, L. Brace, J.D. Winningham, J.D. Craven, N. Maynard and M.A. Hapgood, The cusp: upwelling ion energisation, to be submitted to J. Geophys. Res.
41. M. Lockwood, T.E. Moore, J.H. Waite, Jr., C.R. Chappell, J.L. Horwitz and R.A. Heelis, The geomagnetic mass spectrometer-Mass and energy dispersions of ionospheric ion flows into the magnetosphere, Nature, 316, 612 (1985).
42. R. Tsunoda, R.C. Livingston, C.L. Rino and J.F. Vickrey, Dayside observations of thermal ion upwelling at 800 Km altitude: In ionospheric signature of the cleft ion fountain, EOS, 66 (46), 1003 (1985).
43. D. Roux, J.J. Berthelier, V.A. Gladyshev, L.V. Zinin, V.D. Maslov and M.L. Pivovarov, Vertical transport of  $O^+$  ions at high latitudes, in: Results of the ARCAD-3 Project and of the Recent Programmes in Magnetospheric and Ionospheric Physics, Cepadues ed., Toulouse, 381, (1985).
44. H. Reme, Polar wind and Planetary origin ion escapes at high latitudes, in: Proc. Int. Conf. on Comparative Study of Magnetospheric Systems, LaLonde-des-Maures, France (1985).
45. J.J. Berthelier, Thermal plasma motion in the plasma motion in the polar upper atmosphere, this issue.

46. M. Lockwood, M.O. Chandler, J.L. Horwitz, J.H. Waite, Jr., T.E. Moore and C.R. Chappell, The cleft ion fountain, J. Geophys. Res., 10, 9736 (1985).
47. J.D. Winningham and C. Gurgiolo, DE-2 Photoelectron measurements consistent with a large scale parallel electric field over the polar cap, Geophys. Res. Lett., 9, 977 (1982).
48. J.L. Horwitz and M. Lockwood, The cleft ion fountain: A two-dimensional kinetic model, J. Geophys. Res., 90, 9749 (1985).
49. R.A. Heelis, The effects of interplanetary magnetic field orientation on dayside high latitude ionospheric convection, J. Geophys. Res., 89, 2873 (1984).
50. R.A. Heelis, P.H. Reiff, J.D. Winningham and W.B. Hanson, Ionospheric convection signatures observed by DE2 during northward interplanetary magnetic field, J. Geophys. Res., 91, 5817 (1986).
51. A.W. Yau, E.G. Shelley, W.K. Peterson and L. Lenchyschyn, Energetic auroral and polar ion outflow at DE1 altitudes: Magnitude, composition, magnetic activity dependence, and long-term variations, J. Geophys. Res., 90, 8417 (1985).
52. M. Lockwood, A.P. van Eyken, B.J.I. Bromage, J.H. Waite, Jr, T.E. Moore, J.R. Doupnik, Low energy ion outflows from the ionosphere during a major cap expansion-evidence for equatorward motion of inverted-V structures, this issue.
53. T.E. Moore, J.H. Waite, Jr., M. Lockwood and C.R. Chappell, Observations of coherent ion acceleration in: Proc. Chapman Conf. on Ion acceleration in the ionosphere magnetosphere and Laboratory, Wellesley, USA (1985).
54. R.C. Olsen and C.R. Chappell, Conical ion distributions at one Earth radius - observations from the acceleration region?, this issue.
55. J. Cladis, Parallel acceleration on transport of ions from the polar ionosphere to plasma sheet, Geophys. Res. Lett., in press (1986).
56. D.T. Young, H. Balsiger and J. Geiss, Correlations of magnetospheric ion composition with geomagnetic and solar activity, J. Geophys. Res., 87, 9077 (1982).
57. J.L. Burch, P.H. Reiff and M. Suguira, Upward electron beams measured by DE1: a primary source of dayside region-1 Birkeland currents, Geophys. Res. Lett. 10, 753 (1983).
58. P.B. Dusenbery and L.R. Lyons, Generation of ion-conic distribution by upgoing ionospheric electrons, J. Geophys. Res., 86, 7627 (1981).
59. M. Lockwood, Thermospheric control of the auroral source of  $O^+$  ions for the magnetosphere, J. Geophys. Res., 89, 301 (1984).
60. S.A. Curtis, W.R. Hoegy, L.H. Brace and J.D. Winningham, Cusp altitudinal electron temperature gradient: Dynamics Explorer-2 implications for heating mechanisms, J. Geophys. Res., 90, 4415 (1985).
61. A.R. Barakat and R.W. Schunk, Effect of hot electrons in the polar wind, J. Geophys. Res., 89, 9771 (1984).
62. N. Singh and R.W. Schunk, Temporal behavior of density perturbations in the polar wind, J. Geophys. Res., 90, 6487 (1985).
63. T.I. Gombosi, T.E. Cravens and A.F. Nagy, A time-dependent theoretical model of the polar wind: preliminary results, Geophys. Res. Lett., 12, 167 (1985).
64. M.E. Greenspan, Effects of oblique double layers on upgoing ion pitch angle and gyrophase, J. Geophys. Res., 89, 2842, 1984.
65. T.E. Moore, Acceleration of low-energy Magnetospheric Plasma, this issue.